Ocean Sci. Discuss., 12, C855–C883, 2015
www.ocean-sci-discuss.net/12/C855/2015/

Ocean Science
Discussions
Open Access

Interactive comment on "The open boundary equation" *by* D. Diederen et al.

D. Diederen et al.

d.diederen@student.tudelft.nl

Received and published: 13 October 2015

1. Introduction

We'd like to thank Anonymous Referee #2 for his/her very detailed analysis and contribution to the discussion, which is highly appreciated. As a result, we have had intensive discussions among the authors and have done quite a number of additional numerical experiments to assess the boundary effects. Before we give details on the adjustment length, we provide a summary of our reply, followed by point-to-point replies on specific comments.

2. Summary After some mathematical elaborations, we have been able to demonstrate that the 'Open Boundary Equation' (OBE) also applies to an equilibrium situation (as suggested by Referee #2), which corresponds with the ideal estuary of the linearized case (see section 4.2 of this reply). This is a special hypothetical case where convergence and linearized friction balance out.

However, in this reply, we demonstrate that the adjustment length near the downstream boundary is not due to the adjustment to an "ideal situation" nor to convergence, but purely reflects the distance that the system requires to create over-tides such that the OBE applies. If a wave with the right over-tides is imposed on the downstream boundary, then there is no adjustment required for the OBE to apply. The OBE appears to fit the waves with these specific over-tides very well, whereas it does not fit the pure sinus (in combination with the matching velocity wave that the system generates). This suggests that the OBE accomodates the fully nonlinear solution, intrinsic to the estuary domain, and not the pure sinus of the linearized solution.

3. Response to Part 1

3.1 Validity of Eq. (22)

3.1.1 Numerical issues

Referee #2: *'Indeed, one expects that the authors use a code that will give convergence to the full solution as the discretization is improved (smaller grid size, smalle time step).' (page C606, line 7)*

Referee #2: *'This would indicate that water level and velocity could exhibit a strong gradient near the boundary due to a mismatch between boundary condition and internal solution. This may happen for an elliptic set of equations but not for the hyperbolic system considered here.' (page C606, line 24)*

In consistency theory, Taylor series expansion shows that a higher resolution decreases the discretization errors, where an infinitely small time and space step should lead to the exact governing equations that are approximated. However, convergence to the exact solution is only possible if an exact solution exists (to a semi-infinite channel, forced by a sinusoidal water level at $x = 0$, with the full, nonlinear Saint-Venant equations).

A possible exact solution to this problem has not yet been found and we are not aware of formal methods to prove that it exists. However, we thank Referee #2 for implicitly raising the question of the existence of an exact solution, by referring to numerical convergence theory. Since the answer remains unknown, we should not claim that an exact solution does not exist. That the 'deviations/errors' are numerical errors as a consequence of an artificial solution produced by the numerical model, can indeed not be substantiated. It was just our hunch. We do not think this is the place to enter into a philosophical discussion about the fundamental question of the existence of an exact solution.

The Pearson correlation and the correlation I/J proposed by Referee #2 show a clear seaward boundary effect, which disappears in landward direction, where the correlation becomes nearly complete. The origin of the scatter (Fig. 4, manuscript) is likely the incompatibility of the OBE with the imposed boundary condition in this region. We will elaborate this point in section 4.2. Our hypothesis is that the sinusoidal boundary condition is alien to the estuary domain. However, as a result of the objections of Referee #2, the following statement shall be revised:

Diederen et al.: *'It should be observed that the imposed seaward boundary is not a naturally occurring relationship between water level and flow, and therefore is not consistent with Eq. (22). The disturbance created by the seaward boundary condition requires a certain length for the tidal wave to adjust.' (page 935, line 17)*

Revised: *'It should be observed that the imposed seaward boundary is not compatible with Eq. (22). The deviation from Eq. (22) requires a certain length for the tidal wave to adjust.'*

We have performed simulations where $\beta(x)$ and $Z_x(x)$ varied in space, yielding satisfactory results. However, we now believe that the OBE in theory should only work when all channel characteristics (β, Z_x and K) do not vary in space, which we will elaborate in the interpretation section. We will present simulations with a constant bed slope, which do not show the landward effect observed in simulations with an exponential bed slope.

Diederen et al.: *'There also is a clear effect of the landward boundary, as a result of the weakly reflective numerical boundary condition. For horizontal estuaries, this effect disappears quickly in seaward direction due to channel convergence and friction, but a bed slope severely increases the length of this effect.' (page 935, line 17)*

Revised: *'A minor effect can be observed close to the boundary condition applied landward (Toro, 2001), which is weakly reflective.'*

In order to summarize the results of 100 scenarios, we will present a figure with the results of the correlation I/J, instead of the scatter plot (Fig. 4, manuscript). This figure will show that, for several scenarios, the seaward boundary effect still plays a large role in the inner domain $[0.3L - 07L]$ used in the scatter plot.

Diederen et al.: *'Small values of Eq. (22) demonstrate considerable scatter, which may be explained by numerical errors, which are relatively large in this range.' (page 936, line 11)*

Revision: *As a result of the objections of Referee #2, this statement shall be removed.*

3.1.2 Origin of errors

Referee #2: *'Furthermore I find statements like "From these images it can be concluded that errors/deviations from Eq. (22) enter the domain from the boundaries and travel with the wave celerity." non-balanced as they implictly suggest the validity of Eq. (22) and hence that deviations from it have a numerical origin.' (page c607, line 16)*

With 'errors' we referred to the possibility that Eq. (22) is valid, whereas with 'deviations' we referred to the possibility that Eq. (22) is not valid (so that Eq. (22) is an 'inequality').

Diederen et al.: *'The scatter may be explained by numerical errors, or the scatter may be due to a missing a term in Eq. (22), which would indicate an additional limitation.' (page C412, line 15)*

By writing 'errors/deviations', we kept in the middle whether they are errors or deviations. From here we shall choose the term 'deviations'.

What the 'LHSminusRHS' images (see the supplement to AC455) show is that the 'deviations' mainly enter the domain through the seaward boundary, moving into the domain with a wave-like behavior.

3.1.3 Analytical issues

Another uncertainty problem exists for analytical approximations. Where analytical approximations show disagreement $f_1 = \zeta_t u_x - u_t \zeta_x$ with Eq. (22), two different conclusions can be drawn:

A) The disagreement shows that Eq. (22) is incorrect, deviating from the exact solution, which is analytically approximated.

B) Eq. (22) is correct and the disagreement shows the error in the analytical approximation.

With these two possibilities in mind, we feel that analytical approximations (deviating from the unknown exact solution) cannot be used as formal proof of the (in)correctness of Eq. (22).

Another objection to the analytical counter-example (proposed by Anonymous Referee #2 in section 4.2.3 of RC C423) was illustrated by the 'LHSminusRHS' images (see the supplement to AC455).

Considering time series of $f_1 = \zeta_t u_x - u_t \zeta_x$, the mean μ was subtracted and normalization was applied by dividing by the standard deviation σ:

$f_2 = \frac{f_1 - \mu}{\sigma}$

In the 'LHSminusRHS' images, $f_2(x,t)$ shows that $f_1(x,t)$ is a function of space and time in the numerical model. In the analytical counterexample, $f_1(x)$ it only dependent on space.

The disagreement between the numerical model and the counterexample probably indicates a strong disagreement between the nonlinear equations, used in the numerical model, and the linearized equations, used for the counterexample. Referee #2 mainly discusses the use of linear friction instead of quadratic friction. However, in the linearization also the advection term is removed from the momentum balance and the

water depth is averaged in the mass balance. With these three linearizations, it becomes doubtful if results from the linearized counterexample can be extrapolated to the nonlinear equations, which are the topic of this article.

Finally, by no means do we want to ignore analytical approximations. They are at the basis of this work. But since we consider highly nonlinear scenarios, the article is mainly based on the (fully nonlinear) numerical results.

3.1.4 Presented evidence

Referee #2: *'These ErrorImages (see the supplement to AC455, 'LHSminusRHS') show values of f2 that seem to vary greatly, e.g. the "most linear" cases 21, 24, 65, 74 and 98 show that E varies between roughly -10 and +10 while it should be "small". But what do the authors mean by "small"? When is this variation "small enough" and for which purpose(s)? And why? An in-depth well-motivated discussion on this issue is totally absent. To summarize: the authors claim an (approximate) validity of Eq. (22) that I simply do not see in the ErrorImages.' (page c609, line 12)*

The analysis by f_2 (see Sect. 3.1.3) studies the 'deviations' and how they vary in space and time. In the reply to Referee #2, f_2 was specifically used to indicate a disagreement between the numerical results and the counterexample provided by Referee #2 .

Since the 'deviations' show a wave-like behavior, they have a pathway, so that it can be observed that they (mainly) originate from the seaward boundary. However, f_1 and f_2 by themselves cannot be used to prove the (in)correctness of Eq. (22). Whether f_1 is 'small' or 'big' only has meaning when comparing the size of f_1 to the other two terms, $\zeta_t u_x$ and $u_t \zeta_x$. This was mainly studied in time series, as in Figs. 1-10. f_2 cannot be used to study if the error is large or small, because it is a function of f_1 and is divided by sigma.

We do agree with Referee #2 that near the downstream boundary the deviation is not small, which can be observed in the correlation plots of I/J (see Figs. (1-10)). However, we will demonstrate in Sect 4.2 that these deviations are caused by the imposed boundary, which does not satisfy (22). If a boundary condition is chosen that does approximately satisfy (22), then the deviations become very small.

3.2 The 'Cubature Method' and the 'Tidal Rating Curve'

For the 'Cubature Method', the discharge is measured in the upstream river part. From the location of measurement up to the location of interest, time series of the water level are measured so that the discharge can be spatially integrated, by applying the mass balance.

The 'Tidal Rating Curve' may be directly applied to the location of interest, if Eq. (22) applies at this location. Upstream discharge information is not required. Therefore it is fully local.

We think it is not relevant whether one is 'inferior' or 'superior', since the methods are completely different. Comparison of results would be interesting, once they have been obtained, where the two methods could maybe complement each other.

4. Response to Part 2

4.1 Adopted measure of accuracy

In the article we used the Pearson correlation:

$$\rho(x) = \sum \left(\frac{\left(\zeta_t u_x - \overline{\zeta_t u_x}\right)}{\sqrt{\left(\sum\left(\zeta_t u_x - \overline{\zeta_t u_x}\right)^2\right)}} \frac{\left(u_t \zeta_x - \overline{u_t \zeta_x}\right)}{\sqrt{\left(\sum\left(u_t \zeta_x - \overline{u_t \zeta_x}\right)^2\right)}} \right)$$

where the mean and sum were applied to time series.

For this discussion, we have adopted the method of correlation suggested by Referee #2:

$$\rho_2(x) = I/J$$

$$I = \sqrt{\overline{(\zeta_t u_x - u_t \zeta_x)^2}}\ ,\ J = \min\left(\sqrt{\overline{(\zeta_t u_x)^2}}, \sqrt{\overline{(u_t \zeta_x)^2}}\right).$$

where the mean was applied to time series.

This method is used in Fig. 1-10.

4.2 Amplified and damped estuaries

Referee #2: *'In Part 2 I will explain that the approximate validity of Eq. (22) - if it is found - actually seems to refer to the situation where the tidal wave propagates in a nearly undamped way. In that case, Eq. (22) is approximately satisfied as this is close to the first case from the Appendix of the manuscript. Actually, it is this near-undamped propagation (which is due to a balance between friction and convergence) that is remarkable, and Eq. (22) is merely a property of is. Hence Eq. (22) - if anything - is not so much of an "Open Boundary Equation" as an "Equilibrium Condition". Indeed, Eq. (22) itself is in general rarely satisfied near the boundary.' (page c605, Summary of part 2)*

Referee #2 is right when (s)he indicates that (22) applies to the equilibrium condition of the linearized equations: the "ideal" estuary. We demonstrate this as follows:

In an infinite 'perfect channel' with a constant negative invariant R_2 (see Sect. 2.3 manuscript):

$$u_x = \sqrt{\frac{g}{h}} h_x \longrightarrow h{u_x}^2 = g{h_x}^2$$

so that the OBE follows:

$$\frac{\mathrm{d}h}{\mathrm{d}t} u_x = \frac{\mathrm{d}u}{\mathrm{d}t} h_x$$

Let's take the Lagrangean mass (2.77) and momentum (3.2) balance equations from Savenije (2005):

$$\frac{\mathrm{d}h}{\mathrm{d}t} = -h u_x + \frac{hu}{b}$$

$$\frac{\mathrm{d}u}{\mathrm{d}t} = -g h_x - g Z_x - W$$

This can be modified to become similar to the OBE:

$$\frac{\mathrm{d}h}{\mathrm{d}t}u_x = -hu_x^2 + \frac{hu}{b}u_x$$

$$\frac{\mathrm{d}u}{\mathrm{d}t}h_x = -gh_x^2 - gZ_xh_x - Wh_x$$

When we assume the OBE applies and we take the special case for a frictional and convergent estuary where the negative invariant R_2 is constant in space and time (which can be check by Eq. 5 of the manuscript), the following balance between convergence and friction remains:

$$\frac{hu}{b}u_x = -gZ_xh_x - Wh_x$$

If there is no bed slope, then this simplifies to:

$$\frac{hu}{b}\frac{u_x}{h_x} = -W$$

With the information that the negative invariant R_2 is constant:

$$\frac{hu}{b}\frac{\sqrt{g}}{\sqrt{h}} = W$$

or:

$$\frac{\sqrt{gh}}{b} = \frac{W}{u}$$

This condition is highly unlikely to apply for the nonlinear equations used in the manuscript, where $W = u|u|/(gK^2h^{4/3})$, since the proportionality $(|u| \propto h^{11/6})$ should apply everywhere all the time. However, this is the condition for an ideal estuary in the linearised case (see (2.57) in Savenije (2005)). For this special case, linear friction $W = kuU$ and linearisation of the water depth $(h = \overline{h})$, as applied by Referee #2, lead to a constant velocity amplitude U:

$$U = \frac{\sqrt{g\overline{h}}}{kb}$$

which implies an ideal estuary. Although this is an important finding for ideal estuaries, we can show that the OBE performs well for damped and amplified conditions. We have investigated if the 'deviations', which are mainly found in the 'seaward boundary effect', can be correlated to the amplification/damping of the tidal wave in the estuaries. To answer this question:

1. we have studied more scenarios (see Table 1 and Figs. 1-10),
2. we have compared the correlation I/J to the amplification/damping A_x/A and U_x/U where
   $A(x) = \frac{\max(\zeta)-\min(\zeta)}{2}$, $U(x) = \frac{\max(u)-\min(u)}{2}$,
3. we show time series of $\zeta_t u_x$ versus $u_t\zeta_x$ on several locations in the estuaries,
4. we have studied additional experimental scenarios 5-10, where we imposed a tidal wave on the downstream boundary with the same tidal range as in scenarios 1 and 3, but with the shape of the tidal wave at a location farther in the estuary (see Figs. 11-12)

5. we have used a length scale ψb for the asymptotic tendency of the tidal amplitude to become constant [Cai and Savenije(2013)], where

$$\psi = 1 + \frac{g\eta}{cv \sin\varepsilon} = 1 + \frac{g\eta_0}{cv_0 \sin\varepsilon} = 1 + \frac{1}{{\mu_0}^2} = \frac{1+\mu_0^2}{\mu_0^2}$$

and b is the convergence length of the width. We have compared ψb (see Table 1) to the length scale of adjustment in the correlation plots I/J (see Figs. 1-10).

For the performed scenarios (see Table 1.), we have chosen such parameter values that we obtained a clear amplification and damping, for both low and high amplitude-to-depth ratios. In order to be able to separate the 'seaward boundary effect' from the amplification, we tried to sustain the amplification for a large distance into the estuary.

The correlation plots of I/J have in common that they show a trend towards better performance farther from the seaward boundary. This applies for the all scenarios, amplified or damped.

Except for the 'deviation' near the seaward boundary, the time series of $\zeta_t u_x$ versus $u_t \zeta_x$ show good agreement. This also holds on locations where the tidal dynamics are amplified or damped.

If Eq. (22) would specifically apply for the case where the amplitudes remain constant, as in the first case of the appendix of the manuscript, the optimal performance of I/J should be around the location where the switch from amplification to damping occurs, i.e. where A_x/A and U_x/U are zero. In Scenario #1 this location lies around $x = 0.65L$, and in Scenario #3 this location lies around $x = 0.2L$. Instead of an optimal performance, the correlation I/J shows improving performance landward of this location. The seaward boundary effect is clearly present in these scenarios, especially in the amplified scenarios 1 and 3, allowing some room for doubt.

More clear are the scenarios where a nonlinear shape of the water level was imposed as a seaward forcing boundary condition. The seaward boundary effect has almost

entirely disappeared in scenarios (7,9,10), even though the tidal ranges still show a clear amplification and damping. So for scenarios (7,9,10), there is no boundary effect and the OBE applies in the full reach.

Interestingly, scenarios (9,10) also show a relative damping of the velocity and the tidal amplitude that is almost the same, whereas this is not the case if a pure sinus is imposed at the downstream boundary.

The values of ψb are presented for the 8 scenarios which show amplification and damping in Table 1. When comparing ψb to the length scale of adjustment of the seaward boundary effect in the correlation plots I/J in Fig. 1-10, we observe that ψb is an order of magnitude larger. This comparison confirms that the 'adjustment length' of the seaward boundary effect is not related with the convergence (which is present in the entire domain) nor with an equilibrium between damping and amplification.

In summary, we conclude that the seaward boundary effect is due to the (linear) shape of the imposed sinus, which is not compatible with the (nonlinear) OBE. The OBE requires specific over-tides to apply. The validity of Eq. (22) is not correlated with a 'near-undamped propagation'.

Finally: We are very grateful for the in-depth review by Referee #2, who has forced us to analyze deeper what is behind the apparent (near-)validity of (22). Clearly the last word has not been written about it, and it opens many venues for further analysis. We shall submit a substantially revised paper based on this discussion in due course.

Scenario #	η [m]	Shape BC	$\overline{h}_0$ [m]	b [km]	d [km]	K [m$^{1/3}$ s^{-1}]	L [km]	ψb [km]
1	0.5	Sinus	40	200	∞	70	1800	500
2	0.5	Sinus	40	∞	∞	5	1800	-
3	10	Sinus	40	80	∞	50	1800	400
4	10	Sinus	40	∞	∞	30	1800	-
5	0.5	$0.4L$ (Scen 1.)	40	200	∞	70	1800	500
6	0.5	$0.6L$ (Scen 1.)	40	200	∞	70	1800	500
7	0.5	$0.8L$ (Scen 1.)	40	200	∞	70	1800	500
8	10	$0.1L$ (Scen 3.)	40	80	∞	50	1800	400
9	10	$0.15L$ (Scen 3.)	40	80	∞	50	1800	400
10	10	$0.2L$ (Scen 3.)	40	80	∞	50	1800	400

Table 1. The parameters are displayed of 10 scenarios. In scenario 5-10, the shape of the water level from the indicated location in scenarios 1 and 3 was used as a seaward boundary forcing, after it had been rescaled to the correct amplitude (See Figs. 11,12).

Cai, H. and H. H. G. Savenije (2013), Asymptotic behavior of tidal damping in alluvial estuaries, Journal of Geophysical Research: Oceans, 118(11), 6107–6122, DOI:10.1002/2013JC008772

Interactive comment on Ocean Sci. Discuss., 12, 925, 2015.

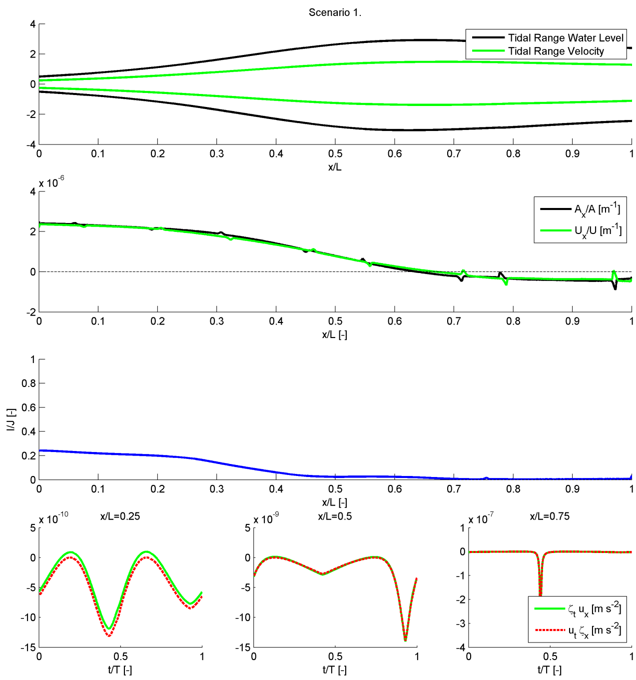

Fig. 1. Scenario 1, parameters are defined in Table 1.

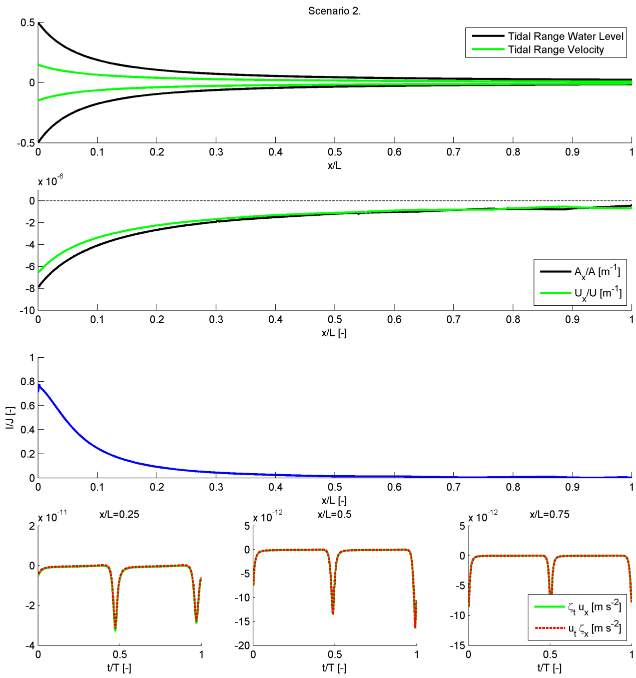

Fig. 2. Scenario 2, parameters are defined in Table 1.

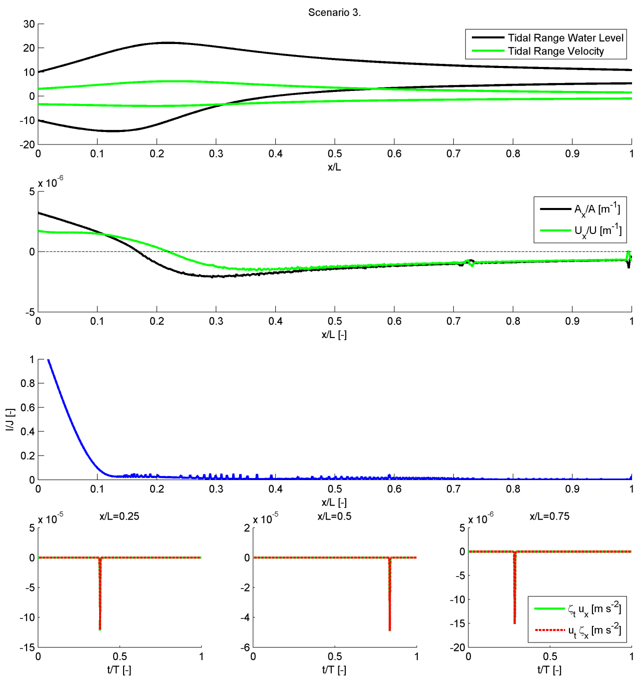

Fig. 3. Scenario 3, parameters are defined in Table 1.

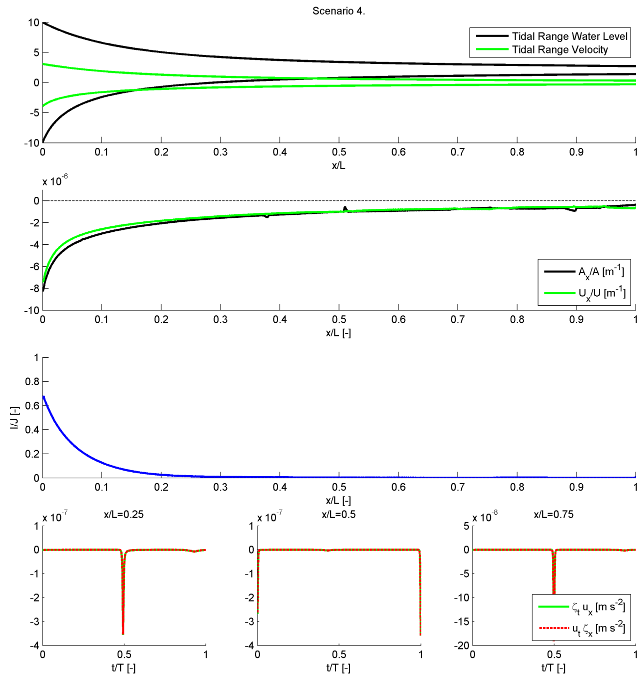

Fig. 4. Scenario 4, parameters are defined in Table 1.

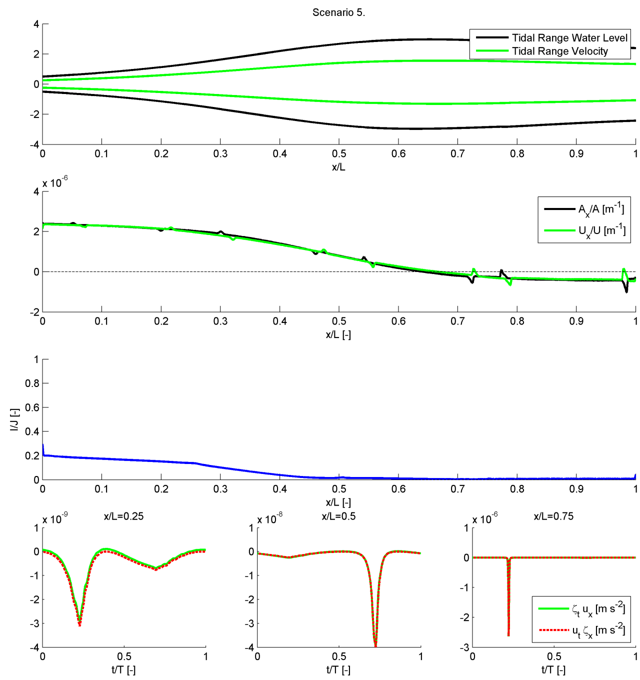

Fig. 5. Scenario 5, parameters are defined in Table 1.

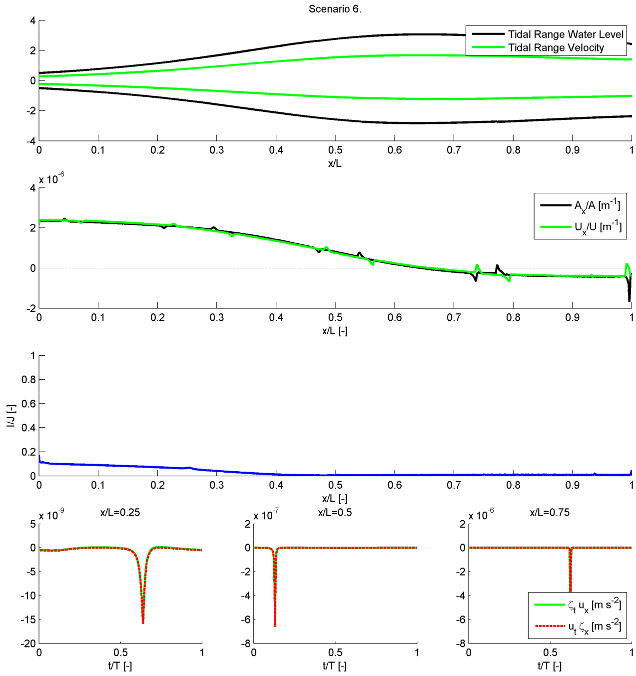

Fig. 6. Scenario 6, parameters are defined in Table 1.

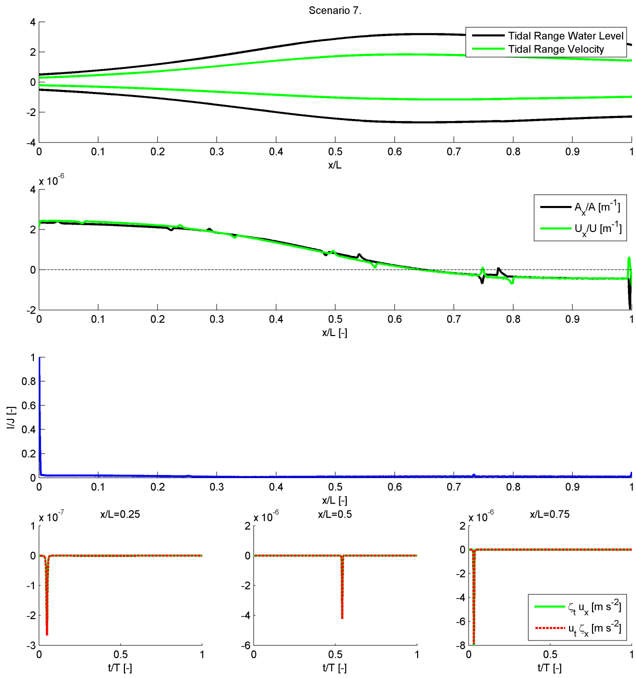

Fig. 7. Scenario 7, parameters are defined in Table 1.

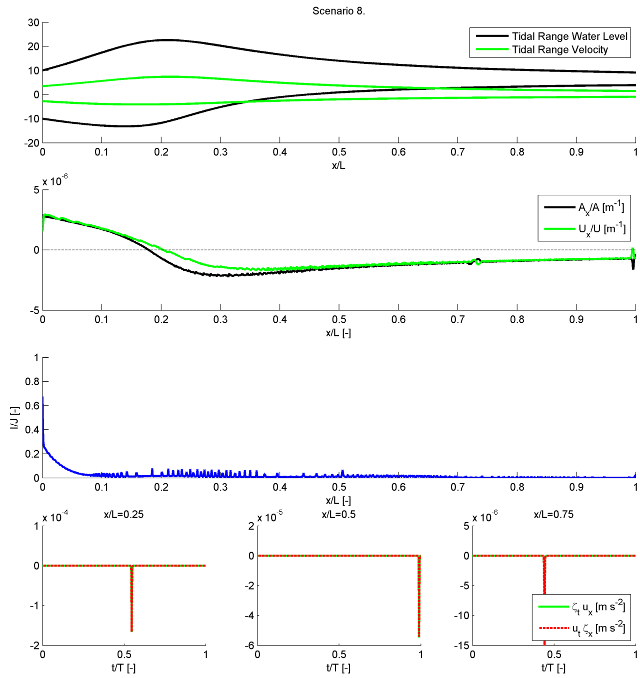

Fig. 8. Scenario 8, parameters are defined in Table 1.

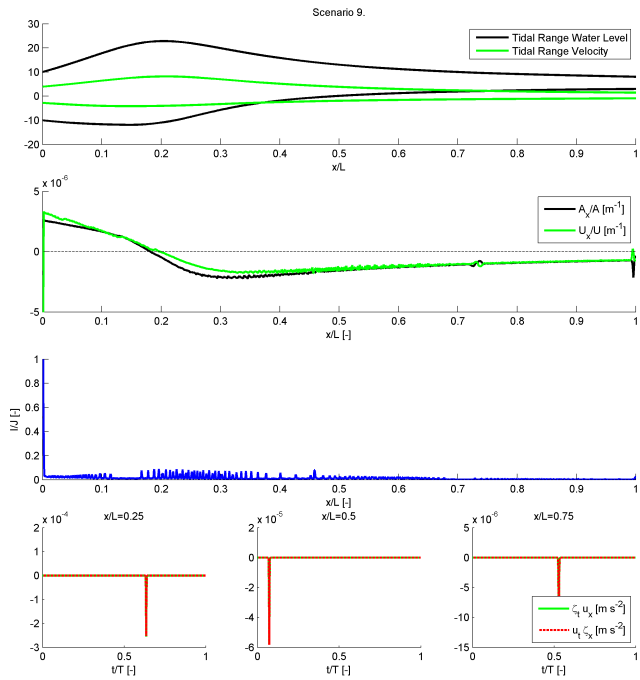

Fig. 9. Scenario 9, parameters are defined in Table 1.

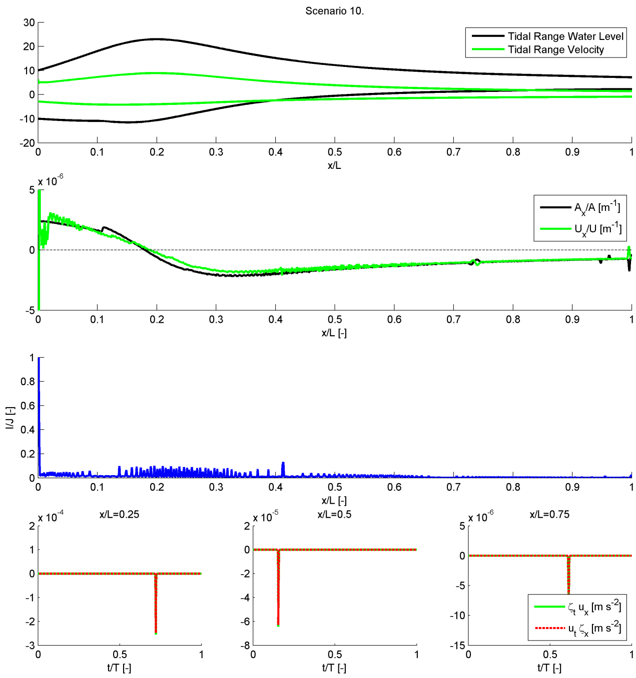

Fig. 10. Scenario 10, parameters are defined in Table 1.

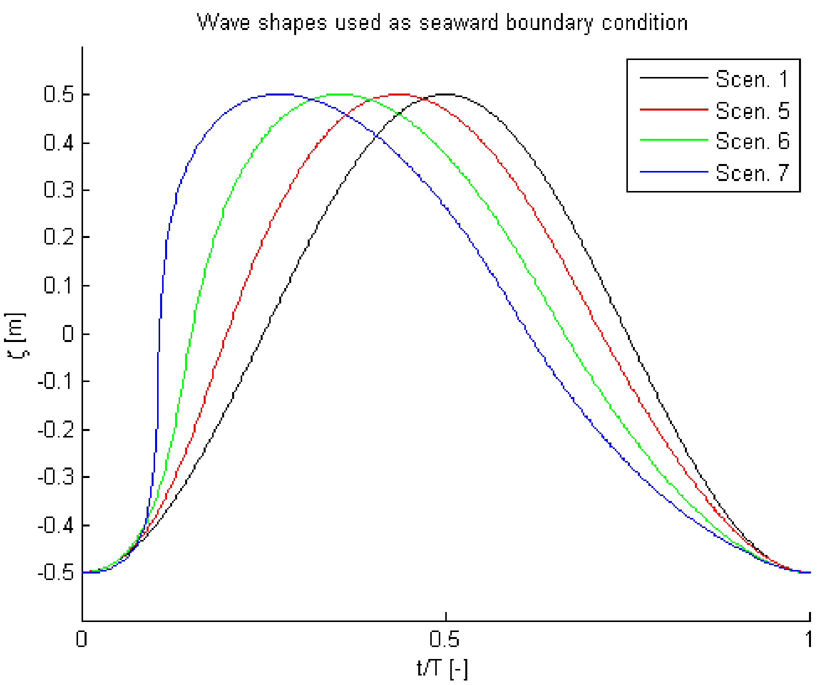

Fig. 11. A comparison of the shape of the seaward boundary condition applied in Scenarios 1, 5, 6 and 7.

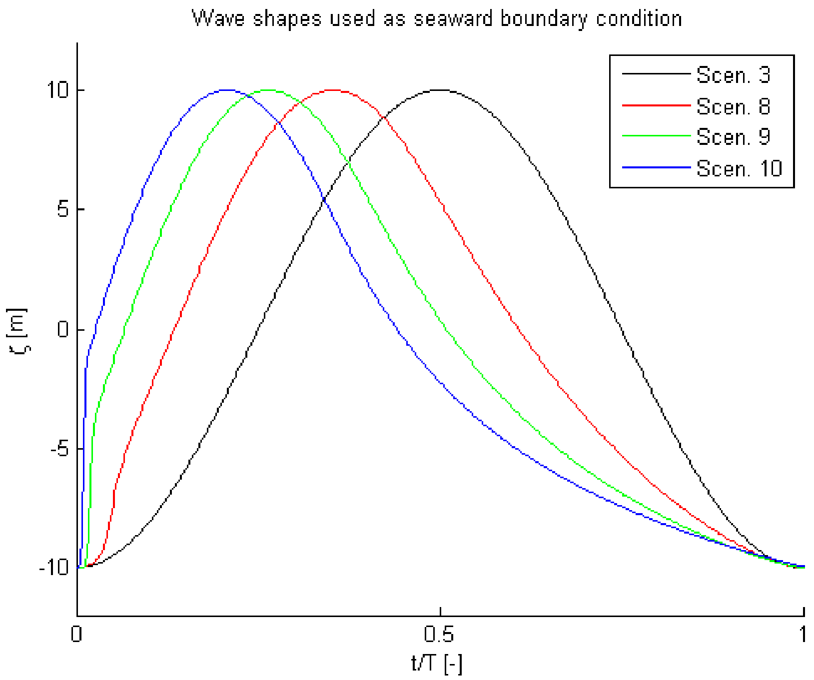

Fig. 12. A comparison of the shape of the seaward boundary condition applied in Scenarios 3, 8, 9 and 10.